

# A label-free approach for detecting vortex-induced vibration using synthetic data augmentation

Sunjoong Kim<sup>1</sup>, Sun-Ho Lee<sup>2</sup>

<sup>1</sup> University of Seoul, Seoul, Korea Rep. [sunjoong@uos.ac.kr](mailto:sunjoong@uos.ac.kr)

<sup>2</sup> University of Seoul, Seoul, Korea Rep. [mundltjsgh@naver.com](mailto:mundltjsgh@naver.com)

## SUMMARY:

Vortex-induced vibrations (VIV) can cause fatigue and degradation of the structural components and lead to visual discomfort for users. Accurate detection and monitoring of VIV are therefore essential. In recent years, advances in machine learning and deep learning have made it possible to detect VIV with reduced human intervention, but the manual labeling process remains a challenge, as it is time-consuming, labor-intensive, and subjective. The label-free approach presented in this study aims to address these challenges by using synthetic data augmentation to generate VIV samples as single-mode harmonics. This approach eliminates the need for manual labeling and point-by-point annotation, making the process much faster and more efficient. The synthetic training data is used to train a deep learning network, which is then used to detect VIVs in real-time using time histories of acceleration. The results of field application demonstrate the effectiveness of this label-free approach in comparison to a prior labeled approach.

*Keywords: Vortex-induced vibrations, Synthetic data augmentation, Signal segmentation, Cable-stayed bridges*

## 1. GENERAL INSTRUCTIONS

Vortex-induced vibrations (VIVs) are significant risks to the stability and vibrational serviceability of long-span bridges (Kim et al., 2017). It can lead to fatigue and degradation of the structural components, as well as visual discomfort to users. Accurate detection and monitoring of VIV are thus crucial for ensuring the long-term reliability and safety of long-span bridges. Machine learning and deep learning advancements have made VIV detection possible with reduced human intervention (Kim and Kim, 2022, Li et al., 2018), but manual labeling remains challenging due to its time-consuming and labor-intensive nature (Lim et al., 2022). Real-time pointwise detection further exacerbates the difficulties by requiring point-by-point annotation (Kim et al., 2023). This study presents a label-free approach using synthetic data augmentation to address these difficulties. Instead of collecting VIV samples, the proposed method generates VIV response data as a single-mode harmonic. The efficacy of the proposed framework is validated using actual datasets of the cable-stayed bridge.

## 2. METHODOLOGY

The proposed framework in this study comprises three essential stages. The first stage encompasses the collection of non-VIV samples, followed by the second stage to synthesize VIV samples based on non-VIV datasets. The last stage involves training a signal segmentation model to classify the time history signals as VIV or non-VIV classes.

## 2.1. Data collection of non-VIV cases

This study utilized the monitoring data of the Jindo Bridge in South Korea. The time histories of vertical acceleration were collected from the accelerometers and ultrasonic anemometer installed at the center of the main span. We selected non-VIV events from the datasets of ordinary wind speeds, lower than lock-in wind speed (10~16 m/s) (Kim et al., 2023). Note that all data points of these cases are annotated as non-VIV, and there are no available VIV samples at this stage.

## 2.2. Synthetic VIV response augmentation

Then, a single-mode vortex-induced vibration (VIV) was synthesized by incorporating artificially generated sine waves into non-VIV samples, which were collected when wind speed was below the onset speed for VIV. The synthesized VIV response, denoted as  $\bar{x}(t)$ , is defined in Equation (1).

$$\bar{x}(t) = \begin{cases} x(t) & (0 < t < T_1) \\ x(t) + A \sin(2\pi f_t t) \times \sin\left(\frac{\pi t}{T_2 - T_1}\right) & (T_1 < t < T_2) \\ x(t) & (T_2 < t < T) \end{cases} \quad (x + a)^n = \sum_{k=0}^n \binom{n}{k} x^k a^{n-k} \quad (1)$$

In Equation (1),  $x(t)$  is the raw acceleration of non-VIV cases,  $T$  is the total measuring time of original data,  $T_1$  and  $T_2$  is the initiation and attenuation time, and  $f_t$  is the frequency of VIVs, respectively.  $A$  is the amplitude of the sinusoidal motion, which was determined to be ten times the standard deviation of  $x(t)$  between  $T_1$  and  $T_2$ . The schematic diagram of the synthesizing process is visualized in Figure 1. As depicted in the second step of the figure, the first and second terms in Equation (1) correspond to the oscillation (gray line) and its envelope (red dotted line), respectively. The ground truth for higher-mode VIV is subsequently defined as the duration between  $t = T_1$  and  $t = T_2$ , represented by the yellow area in the third step.

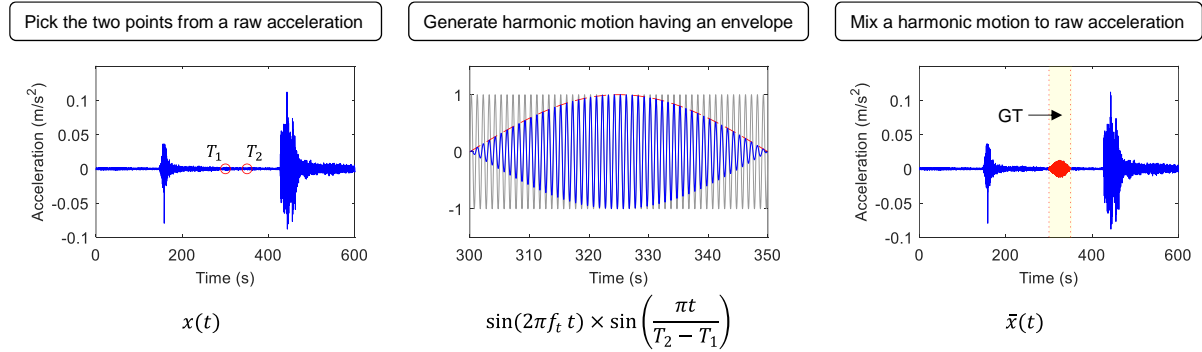


**Figure 1.** The schematic diagram of synthesizing a VIV response

## 2.3. Signal segmentation deep network

Figure 2 illustrates the framework for implementing a signal segmentation deep network. The first step involves the Fourier Synchrosqueezed Transform (FSST) method to extract time-frequency estimates from time histories. This method is chosen for its ability to produce narrow and concentrated time-frequency estimates, improve the readability of time-frequency representations, and outperform other methods in multi-source signal segmentation problems. The next step involves using a Bidirectional Long-Short-Term-Memory (Bi-LSTM) network for sequence-to-sequence classification. The architecture of the proposed Bi-LSTM is as follows.

The input layer receives the FSST, of which size is determined by the frequency resolution of the FSST. The Bi-LSTM layer, which reduces the dimension of the input FSST into a feature number of hidden units, is connected to the input layer. The output from the Bi-LSTM layer is transferred to the fully connected layer of size 3 (the number of classes to be considered), followed by a SoftMax layer that provides score information for every sample point. Finally, the classifier layer estimates the label of sample points based on the scores produced by the SoftMax layer. In this way, the proposed model can classify vibration types in a pointwise manner, effectively determining the difference between VIV and non-VIV.

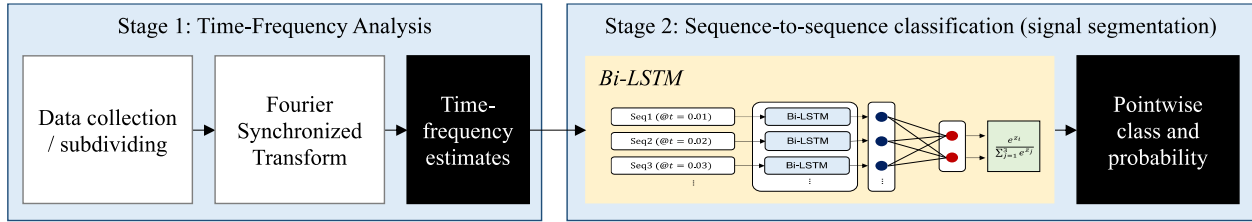
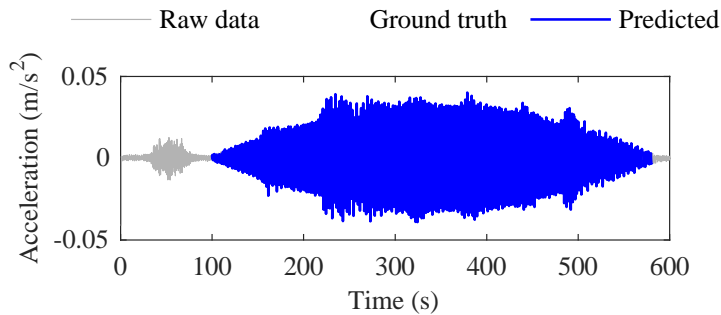


**Figure 2.** The overall process for signal segmentation deep network

### 3. RESULTS AND DISCUSSIONS

#### 3.1. Training results

Figure 3(a) illustrates the representative results of VIV detection, where the ground-truths are represented by the red shaded boxes and the identified results as blue lines. The results clearly demonstrate the effectiveness of the proposed framework in identifying VIV occurrences in a pointwise manner. The confusion matrix shown in Figure 3(b) also confirms the good performance of the deep network model and synthesized datasets for pointwise VIV detection, which resulted in a high accuracy (micro-F1 score) of 98.56%.



(a) Example

True Class	VIV	6,108,737 (39.9%)	160,223 (1.05%)
	Non-VIV	60,417 (0.39%)	8,970,613 (58.6%)
		VIV	Non-VIV
		Predicted Class	

(b) Confusion matrix

**Figure 3.** VIV detection results on the training datasets

#### 3.2. Applicability to actual VIV dataset

The efficacy of the model trained with synthetic data was evaluated by applying it to validation datasets not used in training. For this purpose, labeled data from prior research was employed as validation data (Kim et al., 2023). In comparison, the prior model trained with manually labeled

data achieved a micro-F1 score of around 94%. The label-free approach proposed in this study also demonstrated a satisfactory level of accuracy, with a micro-F1 score of 91%.

Despite this, as seen in Figure 4(a), the label-free model resulted in considerable false positives (FPs) of 8.4%. To delve into this issue, the cases of true positive (TP) and FP are separately presented in Figure 4(b). It is observed in the FP case that the deck exhibited free vibrations after the passage of a vehicle. These free vibrations (non-VIV) were misclassified as VIV because of the synthetic strategy outlined in Section 2.2, which assigned all low-amplitude sinusoids as VIV. Hence, future studies will endeavor to improve the model's performance by incorporating low-amplitude sine waves as negative samples.

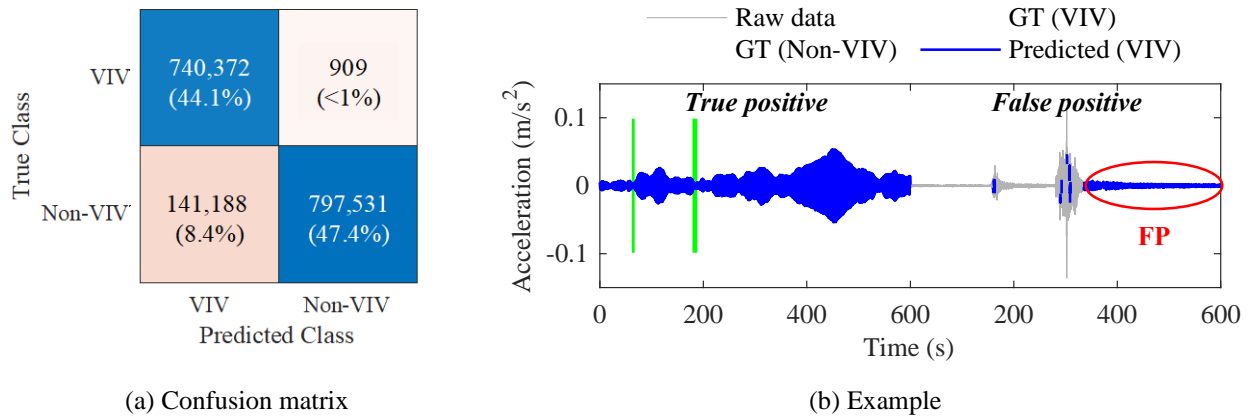


**Figure 4.** VIV detection results on the validation datasets

## 4. CONCLUSIONS

This study presents a label-free approach to detect vortex-induced vibrations (VIVs) in long-span bridges using synthetic data augmentation. The results indicate that the proposed method is effective in detecting VIV in real time with minimal human efforts, contributing to the serviceability assessment of the structure. Further studies are ongoing to increase the method's field applicability and assess its robustness on different bridges.

## ACKNOWLEDGEMENTS

This work was supported by National Research Foundation of Korea (NRF) grants funded by the Korea government (MSIT) [grant numbers RS-2023-00213436].

## REFERENCES

- Kim, S. and Kim, T., 2022. Machine-learning-based prediction of vortex-induced vibration in long-span bridges using limited information. *Engineering Structures*, 266, 114551.
- Kim, S., Lee, S.H. and Kim, S., 2023. Pointwise multiclass vibration classification for cable-supported bridges using a signal-segmentation deep network. *Engineering Structures*, 279, 115599.
- Kim, S., Park, J. and Kim, H.K., 2017. Damping identification and serviceability assessment of a cable-stayed bridge based on operational monitoring data. *Journal of Bridge Engineering*, 22(3), 04016123.
- Li, S., Laima, S. and Li, H., 2018. Data-driven modeling of vortex-induced vibration of a long-span suspension bridge using decision tree learning and support vector regression. *Journal of Wind Engineering and Industrial Aerodynamics*, 172, 196-211.
- Lim, J., Kim, S. and Kim, H.K., 2022. Using supervised learning techniques to automatically classify vortex-induced vibration in long-span bridges. *Journal of Wind Engineering and Industrial Aerodynamics*, 221, 104904